

SIGNATURES OF QCD MATTER AT RHIC

H. HEISELBERG

*NORDITA, Blegdamsvej 17
DK-2100 Copenhagen Ø., DENMARK
E-mail: hh@nordita.dk*

A. D. JACKSON

*Niels Bohr Institute, Blegdamsvej 17
DK-2100 Copenhagen Ø., DENMARK
E-mail: jackson@nbi.dk*

We discuss possible experimental signatures of forming a Quark-Gluon plasma in high energy nuclear collisions. In first order phase transitions such as the chiral symmetry restoration supercooling may lead to density fluctuations such as droplet formation and hot spots. These will lead to rapidity fluctuations event-by-event and triggering on such fluctuations will have distinct effects for HBT radii.

1 Introduction

Results from the RHIC collider next year are eagerly awaited. The hope is to observe the phase transition to quark-gluon plasma, the chirally restored hadronic matter and/or deconfinement. This may be by distinct signals of J/Ψ suppression, strangeness enhancement, η' enhancement, enhanced temperature and multiplicity fluctuations¹, etc. Other signals are plateau's in temperatures, transverse flow or other collective quantities as function of centrality, transverse energy or multiplicity. We will here suggest other signals of a first order phase transition namely rapidity fluctuations and associated variations in HBT radii.

2 Supercooling and Droplet formation

Lattice calculations suggest that QCD has a first order transition at zero chemical potential provided that the strange quark is sufficiently light². Recent work using random matrix theory (RMT)³ suggests an effective thermodynamic potential of the form

$$\Omega(\phi)/N_f = \phi^2 - \frac{1}{2} \ln\{[\phi^2 - (\mu + iT)^2] \cdot [\phi^2 - (\mu - iT)^2]\} . \quad (1)$$

The value of $\phi \sim \langle \bar{\psi}\psi \rangle$ at the minima of $\Omega(\phi)$ is related to the expectation value of the quark condensate which is the order parameter for chiral symmetry breaking. Minimization of Eq.(1) leads to a fifth order polynomial equation for ϕ which is identical in form to the results of Landau-Ginzberg theory using a ϕ^6

potential. One solution to this equation corresponds to the restored symmetry phase with $\phi = 0$. This model predicts a second order transition for $\mu = 0$ at a temperature, T_c , which is generally agreed to be approximately 140 Mev. For $T = 0$, a first order transition occurs at some μ_0 . Since the phases in which chiral symmetry is broken and restored must be separated in the (μ, T) plane by an unbroken line of phase transitions, this implies the existence of a tricritical point. In this model, the tricritical point is at

$$\frac{T_3}{T_c} = \frac{1}{2}\sqrt{\sqrt{2} + 1} \quad \text{and} \quad \frac{\mu_3}{\mu_0} \approx 0.610 .$$

Further, the discontinuity in the density at $(T = 0, \mu_0)$ can be estimated as $\Delta n \approx 2.5n_0$ where n_0 is the equilibrium density of nuclear matter. An inevitable consequence of such a phase diagram is the existence of spinodal lines within which $\Omega(\phi)$ has three local minima. In this region, nuclear matter can be either superheated or super cooled.

The qualitative features of this phase diagram lead to an interesting scenario for relativistic heavy ion collisions in which matter is compressed and heated. Some or all of this matter will undergo chiral restoration. If the subsequent expansion is sufficiently rapid, matter will pass the phase coexistence curve with little effect since the restored symmetry phase with $\phi = 0$ will remain a local minimum of $\Omega(\phi)$. This suggests the possible formation of “droplets” of supercooled chiral symmetric matter with relatively high baryon and energy densities in a background of low density broken symmetry matter. These droplets can persist until the system reaches the spinodal line and then return rapidly to the now-unique broken symmetry minimum of $\Omega(\phi)$. The schematic nature of Eq.(1) makes it impossible to make quantitative predictions about the properties of such droplets. (The effective thermodynamic potential can well have additional terms which are independent of ϕ .) However, a large mismatch in density and energy density seems to be a robust prediction. Note that these “droplets” are kinematically distinct from the “hot spots” usually associated with jets and minijets⁴. Jets are characterized by a strong directional orientation and a high transverse momentum not expected for the present droplets.

Such density fluctuations can occur only for first order transitions. In the RMT model, these will only be the case for sufficiently high net baryon densities. In ultrarelativistic nuclear collisions at mid rapidity, the baryon density is low as in the early universe and, according to RMT, the transition is of second order. One should then investigate nuclear fragmentation regions or go to lower collision energies (e.g., AGS energies) to observe droplet formation. However, most lattice simulations do find a first order transition at zero baryon

density.

3 Rapidity Fluctuations

If the transitions is first order, matter may supercool and subsequently create fluctuations in a number of quantities. Density fluctuations in the form of hot spots or droplets of dense matter with hadronic gas in between is a likely outcome. We shall refer to these regions of dense and hot matter in space-time as well as in momentum space as droplets. If we assume that hadrons emerge as a Boltzmann distribution with temperature T from each droplet and ignore transverse flow, the resulting particle distribution is

$$\frac{dN}{dyd^2p_\perp} \propto \sum_i f_i e^{-m_\perp \cosh(y-\eta_i)/T}. \quad (2)$$

Here, y is the particle rapidity and p_\perp its transverse momentum, f_i is the number of particles hadronizing from each droplet i , and

$$\eta_i = \frac{1}{2} \log \frac{t_i + z_i}{t_i - z_i} = \frac{1}{2} \log \frac{1 + v_i}{1 - v_i} \quad (3)$$

is the rapidity of droplet i .

When $m_\perp/T \gg 1$, we can approximate $\cosh(y - \eta_i) \simeq 1 + \frac{1}{2}(y - \eta_i)^2$ in Eq.(2). The Boltzmann factor determines the width of the droplet rapidity distribution as $\sim \sqrt{T/m_\perp}$. The rapidity distribution will display fluctuations in rapidity event by event when the droplets are separated by rapidities larger than $|\eta_i - \eta_j| \gtrsim \sqrt{T/m_\perp}$. If they are evenly distributed by smaller rapidity differences, the resulting rapidity distribution (2) will appear flat.

The droplets are separated in rapidity by $|\eta_i - \eta_j| \sim \Delta z/\tau_0$, where Δz is the correlation length in the dense and hot mixed phase and τ_0 is the invariant time after collision at which the droplets form. Assuming that $\Delta z \sim 1\text{fm}$ — a typical hadronic scale — and that the droplets form very early $\tau_0 \lesssim 1\text{fm}/c$, we find that indeed $|\eta_i - \eta_j| \gtrsim \sqrt{T/m_\perp}$ even for the light pions.

If strong transverse flow is present in the source, the droplets may also move in a transverse direction. In that case the distribution in p_\perp may be non-thermal and azimuthally asymmetric.

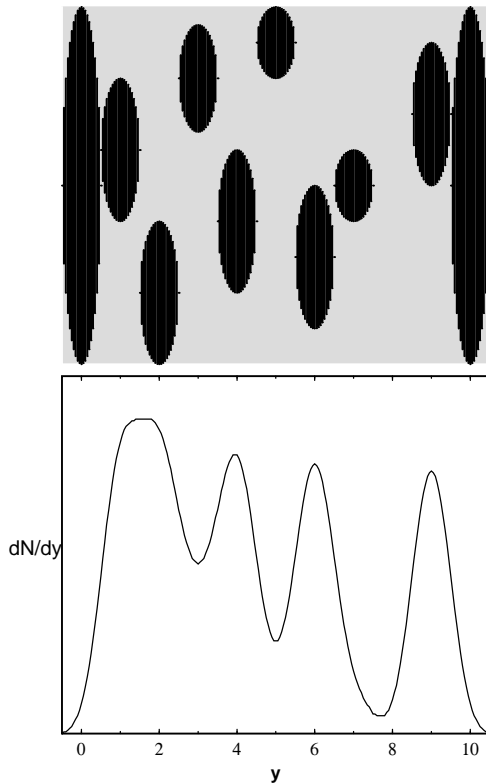


Figure 1: Droplet formation (top) and corresponding rapidity distribution (bottom).

4 HBT and Correlation Functions

In this section we briefly review the correlation function analysis of Bose-Einstein interference. For details we refer to references on stellar intensity interferometry⁵, pion interferometry in pp⁶ and AA collisions^{7,8,9}.

For a source of size R we consider two particles emitted a distance $\sim R$ apart with relative momentum $\mathbf{q} = (\mathbf{k}_1 - \mathbf{k}_2)$ and average momentum, $\mathbf{K} = (\mathbf{k}_1 + \mathbf{k}_2)/2$. Typical heavy ion sources in nuclear collisions are of size $R \sim 5$ fm, so that interference occurs predominantly when $q \lesssim \hbar/R \sim 40$ MeV/c. Since typical particle momenta are $k_i \gtrsim K \sim 300$ MeV/c, the interfering particles travel almost parallel, i.e., $k_1 \simeq k_2 \simeq K \gg q$. The correlation function due

to Bose-Einstein interference of identical particles from an incoherent source is (see, e.g.,⁹)

$$C_2(\mathbf{q}, \mathbf{K}) = 1 \pm \left| \frac{\int d^4x S(x, \mathbf{K}) e^{iqx}}{\int d^4x S(x, \mathbf{K})} \right|^2, \quad (4)$$

where $S(x, \mathbf{K})$ is the source distribution function describing the phase space density of the emitting source. The $+/-$ refers to boson/fermions respectively.

Experimentally the correlation functions for identical mesons ($\pi^\pm\pi^\pm$, $K^\pm K^\pm$, etc.) are often parametrized by the gaussian form

$$C_2(q_s, q_o, q_l) = 1 + \lambda \exp \left[-q_s^2 R_s^2 - q_o^2 R_o^2 - q_l^2 R_l^2 - 2q_o q_l R_{ol}^2 \right]. \quad (5)$$

Here, $\mathbf{q} = \mathbf{k}_1 - \mathbf{k}_2 = (q_s, q_o, q_l)$ is the relative momentum between the two particles and $R_i, i = s, o, l$ the corresponding sideward, outward and longitudinal HBT radii respectively. We have suppressed the \mathbf{K} dependence. We will employ the standard geometry, where the *longitudinal* direction is along the beam axis, the *outward* direction is along \mathbf{K} , and the *sideward* axis is perpendicular to these. Usually, each pair of mesons is lorentz boosted longitudinal to the system in which their rapidity vanishes, $Y = 0$. Their average momentum \mathbf{K} is then perpendicular to the beam axis and is chosen as the outward direction. In this system the pair velocity $\beta_{\mathbf{K}=\mathbf{K}/E_K}$ points in the outward direction with $\beta_o = p_\perp/m_\perp$ where $m_\perp = \sqrt{m^2 + p_\perp^2}$ is the transverse mass. Often models assume a boost invariant source and boost to the cms where $Y = 0$ where a number of boost factors disappear and the out-longitudinal coupling R_{ol} vanishes. The reduction factor λ in Eq.(5) may be due to long lived resonances^{8,10}, coherence effects, incorrect Gamow corrections¹¹ or other effects. It is found to be $\lambda \sim 0.5$ for pions and $\lambda \sim 0.9$ for kaons.

5 HBT for Droplets

Droplets lead to spatial fluctuations in density which can be probed by correlations between identical particles⁵. For simplicity we parametrize these droplets by spatial and temporal gaussians of size R_d and duration of emission t_d . The distribution of particles in space and time — usually referred to as the source — for droplets situated at $x_i = (\mathbf{r}_i, t_i)$ is

$$S(x, K) \sim \sum_i \tilde{S}(x_i, K) \exp \left[-\frac{(\mathbf{r} - \mathbf{r}_i)^2}{2R_d^2} - \frac{(t - t_i)^2}{2t_d^2} \right], \quad (6)$$

where $\tilde{S}(x_i, K)$ is the distribution of sources. Normalizations of S cancel when calculating correlation functions, Eq.(4). Other effects as transverse flow, opacities¹², resonances¹⁰, etc. can be included but we shall ignore them here for

simplicity. Likewise, the extension to droplets of different size and duration of emission is straight forward but unnecessary for our purpose. We expect the scale of \tilde{S} is the nuclear overlap size R_A of order several *fermi*'s whereas the droplet size R_d is smaller — of order a few *fermi*'s.

From (4) and (6) we obtain

$$C_2(q) \simeq 1 + \exp[-\mathbf{q}^2 R_d^2 - (\mathbf{q} \cdot \beta)^2 t_d^2] |\tilde{S}(q, K)|^2, \quad (7)$$

where

$$\tilde{S}(q, K) = \sum_i \tilde{S}(x_i, K) e^{iq \cdot x_i} / \sum_i \tilde{S}(x_i, K) \quad (8)$$

is the Fourier transform of the distribution of sources and $\beta = \mathbf{K}/K_0$ is the average velocity of the pair.

If there is only a single droplet $\tilde{S}(q, K) = 1$ and the correlation function is simply given by the droplet gaussian. If there are many droplets, the sum can be replaced by an integral.

5.1 Non-expanding Sources

For non-expanding sources we can assume that the particle momentum distribution is the same for all droplets, i.e., independent of \mathbf{K} .

For many droplets we assume that the droplets are distributed by a gaussian

$$\tilde{S}(x_i, K) \sim \exp(-\mathbf{r}_i^2/2R_A^2 - t_i^2/2R_A^2), \quad (9)$$

where t_A is the spread in droplet formation times and R_A is the size of the nuclear overlap zone. It increases with decreasing impact parameter - roughly as $R_A(b) \simeq \sqrt{R_A(0)^2 - b^2}$, where $R_A(0) \simeq 1.2A^{1/3} fm$ is the nuclear size.

The resulting correlation function becomes

$$C_2(q) \simeq 1 + \exp[-\mathbf{q}^2 (R_A^2 + R_d^2) - (\mathbf{q} \cdot \beta)^2 (t_A^2 + t_d^2)]. \quad (10)$$

Since R_A and ct_A are typically of nuclear scales $\sim 5 - 10$ fm whereas we expect $R_d \sim 1$ fm, the droplets are simply “drowned” in the background of the other droplets.

In the case of only two droplets (of same size) the resulting correlation function is

$$C_2(q) \simeq 1 + \exp[-\mathbf{q}^2 R_d^2 - (\mathbf{q} \cdot \beta)^2 t_d^2] \cos\left(\frac{1}{2} q \cdot (x_1 - x_2)\right). \quad (11)$$

However, as the x_i 's differ from event to event the oscillation in (11) will, when summing over events, result in a Fourier transform over the distribution

of x_i 's in different event and the end result will be similar to (10). The number of pairs in a single event at RHIC energies is probably not large enough to do event-by-event HBT. The oscillation will also be smeared by resonances, Coulomb effects, a hadronic background, etc.

We conclude that it will be very difficult to see the individual droplets through HBT when the sources do not expand.

5.2 Expanding Sources

At RHIC energies the collision regions are rapidly expanding particularly in the longitudinal direction. Consequently the droplets may have different expansion velocities and rapidities and the distribution $\tilde{S}(x_i, K)$ will depend on K and this difference will now be exploited.

When the droplets are separated in rapidity such that $|\eta_i - \eta_j| \gtrsim \sqrt{T/m_\perp}$, only particles within the same droplet contribute to the correlation function. If we transform to the droplet center-of-mass system, i.e. $\eta_i = 0$, the correlation function is then given by (10) with $\tilde{S} = 1$. In terms of q_s, q_o, q_l it can be written

$$C_2(q) = 1 + \exp \left[-q_s^2 R_d^2 - q_o^2 (R_d^2 + \beta_o^2 t_d^2) - q_l^2 (R_d^2 + \beta_l^2 t_d^2) - 2q_o q_l \beta_o \beta_l t_d^2 \right], \quad (12)$$

where $\beta_o = p_\perp/m_\perp \cosh(Y)$ and $\beta_l = \tanh(Y)$, are the transverse (outward) and longitudinal velocities respectively of the pair.

When the droplets overlap in rapidity, we need to consider the distribution of droplets in more detail. At ultrarelativistic energies the rapidity distribution is expected to display approximate Bjorken scaling, i.e., the rapidity distribution is approximately given by (2) where the droplet rapidities η_i are more or less evenly distributed between target and projectile rapidities. Parametrizing the transverse and temporal distribution as gaussians, we arrive at the droplet distribution

$$\tilde{S}(x_i, K) \sim \exp \left[-\frac{m_\perp}{T} \cosh(Y - \eta_i) - \frac{\mathbf{r}_{\perp,i}^2}{2R_A^2} - \frac{(\tau_i - \tau_f)^2}{2t_A^2} \right], \quad (13)$$

where $\tau_i = \sqrt{t_i^2 - z_i^2}$ is the invariant time and τ_f the average freeze-out time.

The resulting correlation function becomes (in the system $Y = 0$, where $\beta_l = \tanh Y = 0$ and $\beta_o = p_\perp/m_\perp$)

$$C_2(q) = 1 + \exp \left[-q_s^2 (R_A^2 + R_d^2) - q_o^2 (R_A^2 + R_d^2 + \beta_o^2 (t_A^2 + t_d^2)) - q_l^2 \left(\tau_f^2 \frac{T}{m_\perp} + R_d^2 \right) \right]. \quad (14)$$

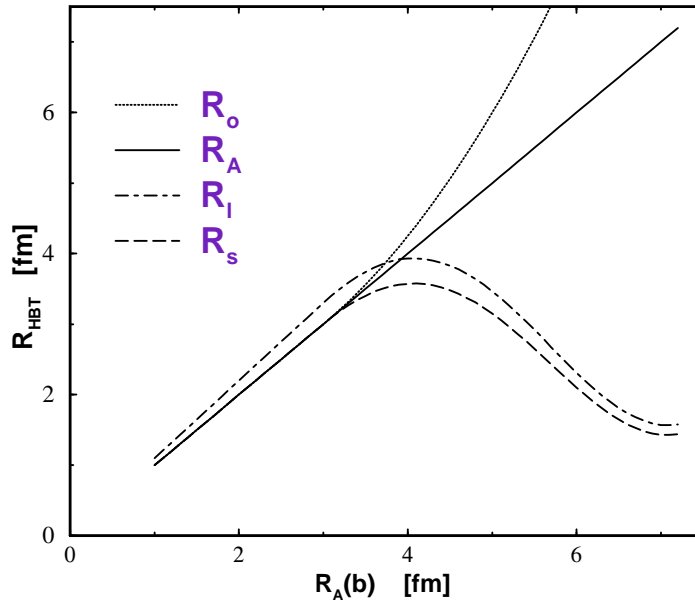


Figure 2: The HBT radii as function of nuclear overlap R_A which is proportional to centrality, dN/dy or E_{\perp} . Droplet formation is assumed to set from semicentral collisions. A long mixed phase will then lead to large outward HBT radius R_o whereas triggering on large rapidity fluctuations corresponding to small droplets leads to smaller longitudinal R_l and sideward R_s HBT radii.

We observe that the larger nuclear size R_A dominates the smaller droplet size R_d when droplets overlap.

6 Centrality dependence of HBT radii

We can now study the consequences of forming droplets at RHIC energies. The onset of large rapidity fluctuations is one signal but it should be accompanied by the following behavior of the HBT radii. In peripheral collisions, where the nuclear overlap and stopping is small, we do not expect sufficient energy densities to build up and form droplets. Thus the HBT radii should simply grow with the size of the geometrical nuclear overlap, centrality, dN/dy and transverse energy E_T . At SPS energies the HBT radii are indeed found to scale

approximately with the geometrical sizes of the colliding systems as given by (14).

If energy densities achieved in RHIC collisions are sufficient to form droplets in central collisions, the HBT radii will deviate from the geometrical overlap if triggered on large rapidity fluctuations (see Fig. 2) as given by Eq.(12). Comparing the theoretical predictions of Eqs. (12) and (14) with the experimentally measured HBT radii of Eq.(5) we see that the sideward and longitudinal HBT radii decrease from the nuclear size R_A, t_A to the droplet sizes R_d, t_d . Thus at a certain semi-centrality, where energy densities achieved in nuclear collisions start becoming large enough to create droplets, the sideward and longitudinal HBT radii should bend over and start decreasing with centrality. The outward HBT radius may behave differently depending on the duration of emission. The droplets may emit hadrons for a long time, as is the case for a long lived mixed phase (referred to as the “burning log”). In the hydrodynamic calculation of Ref. ¹³), the duration of emission and consequently the outward HBT radius increase drastically up to five times larger than the transverse size of the system, i.e. R_A . This scenario is indicated in Fig. 2.

Besides droplets we may expect some hadronic background. It is straight forward to include such one in the correlation function. As its spatial extend is expected to be on the scale $\sim R_A$, it will reduce the correlation function at small $q \sim \hbar/R_A$. However, the droplets will still lead to correlations at large relative momenta of order $q \sim \hbar/R_d$. The large q correlations are suppressed by the square of the fraction of pions emerging from droplets at a given rapidity.

7 Summary

If first order transitions occur in high energy nuclear collisions, density fluctuations are expected which may show up in rapidity fluctuations event-by-event. HBT interferometry adds an important space-time picture to the purely momentum space information one gets from single particle spectra. Triggering on rapidity fluctuations, the HBT radii may display a curious behavior. The outward HBT radius R_o may increase drastically with centrality due to a long lived mixed phase. The longitudinal R_l and sideward R_s HBT radii will, however, saturate and *decrease* for the very central collisions because a large rapidity fluctuation signals a hot and dense droplet of small size.

The predicted behavior for the sideward and longitudinal HBT radii is *opposite* to that predicted in cascade and hydrodynamic calculations. It would be a clean signal of a first order phase transition in nuclear collisions.

References

1. M. Stephanov, K. Rajagopal, E. Shuryak, hep-ph/9806219.
2. Y. Iwasaki, K. Kanaya, S. Kaya, S. Sakai, T. Yoshi, *Phys. Rev. D* **54**, 7010 (1996).
3. M.A. Halasz, A.D. Jackson, R.E. Shrock, M.A. Stephanov, J.J.M. Verbaarschot, hep-ph/9804290.
4. M. Gyulassy, D. H. Rischke, B. Zhang *Nucl.Phys. A* **613**, 397 (1998).
5. R. Hanbury–Brown and R.Q. Twiss, *Phil. Mag.* **45**, 633 (1954).
6. G. Goldhaber, S. Goldhaber, W. Lee, and A. Pais, *Phys. Rev.* **120**, 300 (1960); S.E. Koonin, *Phys. Lett. B* **70**, 43 (1977).
7. M. Gyulassy, S. K. Kaufmann and L. W. Wilson, *Phys. Rev. C* **20**, 2267 (1979).
8. T. Csörgő and B. Lörstad, *Phys. Rev. C* **54**, 1390 (1996).
9. S. Chapman, J.R. Nix, and U. Heinz, *Phys. Rev. C* **52**, 2694 (1995). B. Tomasik and U. Heinz, nucl-th/9805016.
10. H. Heiselberg, *Phys. Lett. B* **379**, 27 (1996). U.A. Wiedemann, U. Heinz, *Phys. Rev. C* **57** (1998) 266.
11. G. Baym and P. Braun-Munzinger, *Nucl. Phys. A* **610**, 286c (1996).
12. H. Heiselberg and A.P. Vischer, *Eur. Phys. J. C* **1**, 593 (1998); *Phys. Lett. B* **421**, 18 (1998).
13. S. Bernard, D. Rischke, J. Maruhn, W. Greiner, nucl-th/9703017.